Vol 11 No 7, July 2002
1009-1963/2002/11(07)/0730-07

Chinese Physics

© 2002 Chin. Phys. Soc.
and IOP Publishing Ltd

Surface optical phonon-assisted electron Raman scattering in a semiconductor quantum disc*

Liu Cui-Hong(刘翠红)[a)b)] †, Ma Ben-Kun(马本堃)[a)], and Chen Chuan-Yu(陈传誉)[b)]

[a)] *Department of Physics and Institute of Theoretical Physics, Beijing Normal University, Beijing* 100875, *China*

[b)] *Department of Physics, Guihuagang Campus, Guangzhou University, Guangzhou* 510405, *China*

(Received 19 September 2001; revised manuscript received 25 March 2002)

We have carried out a theoretical calculation of the differential cross section for the electron Raman scattering process associated with the surface optical phonon modes in a semiconductor quantum disc. Electron states are considered to be confined within a quantum disc with infinite potential barriers. The optical phonon modes we have adopted are the slab phonon modes by taking into consideration the Fröhlich interaction between an electron and a phonon. The selection rules for the Raman process are given. Numerical results and a discussion are also presented for various radii and thicknesses of the disc, and different incident radiation energies.

Keywords: Raman scattering, surface optical phonon modes, quantum disc
PACC: 7830, 7320D, 6320K

1. Introduction

Recently, the nanometre-scale crystallites of semiconductor materials have attracted much attention because of their relevance for practical applications and as probes for the study of the electronic structure of mesoscopic media.[1−16] Most of the theoretical studies of quantum dots (QDs) are focused on spherical QDs. As a matter of fact, the shapes of QDs depend on the growth conditions. It can be not only an ideal spherical dot, but also a pyramid, disc or cone.[9−13] In this paper, we discuss the disc-like QD with a lateral size much larger than the extent in the growth direction.

One of the major issues about QDs remaining to be addressed concerns the effect of the phonon on the electron, hole and exciton. More and more works have shown that the electron–phonon interaction plays an important role in determining the physical properties of nanocrystals especially for low-dimensional structures.[13−19] Many authors have not only considered the effect of bulk longitudinal optical (LO) and transverse optical (TO) phonon modes but also the surface optical (SO) phonon modes and interface optical (IO) phonon modes.[13−17]

It is well known that the Raman scattering experiment is a powerful tool to obtain information such as electronic structure and electron–phonon interaction in low-dimensional semiconductor materials. Experimental research on the Raman scattering in nanocrystals has been extensively reported.[27,28,33−36] Many theoretical attempts to interpret experimental results usually focus on the calculation of the differential cross section for Raman scattering. Bergues *et al*[20] discussed the differential cross section for electron Raman scattering in quantum well (QW) wires and free-standing wires involving phonon-assisted transition at T=0K. Zucker *et al*[21] studied the Raman scattering process in GaAs/$Al_xGa_{1-x}As$ QWs. Cardona *et al* discussed the Raman scattering in QWs under high magnetic fields[22] and electric fields.[23] Krauss and Wise[24] worked out the multiphonon resonant Raman scattering (RRS) in PbS QDs. Sood *et al*[25,26] first reported the IO modes in GaAs–AlAs superlattices by Raman scattering. Using this Raman scattering method, Hayashi and Kanamori[27] have demonstrated that the surface phonon mode appears between the LO and TO phonon modes in GaP microcrystals. Liu *et al*[28] have reported the surface phonon mode in a non-polar microcrystal. As far as we know, however, little attention has been paid to similar work in polar crystals. Cardona and coworkers studied the first-order Raman cross section and the resonance profile for optical phonons in semiconductor spherical QDs.[30,31] The phonon modes they discussed are neither purely LO nor purely SO

*Project supported by the Natural Science Foundation of Guangdong Province, China (Grant No 980378)
†E-mail address: cychen@guangztc.edu.cn

modes, but a mixture of LO, TO and SO components. In this paper, we calculate the first-order Raman scattering process in a QD, involving the transition assisted by SO phonons and photons.

In this paper we first outline the model and theory. In section 2 we give the Hamiltonian, the relevant eigenfunctions and eigenenergy levels of the system to be studied. In section 3, we derive the analytical expressions of the differential cross section for the resonant Raman scattering in SO phonon modes. We also study the selection rules for the Raman scattering processes in this section. Numerical calculation and discussion with a typical GaAs QD are given in section 4, and finally a brief summary is presented in section 5.

2. Model and theory

We describe briefly the model and the theory applied in our studies. We consider a polar crystal QD (Fig.1), with electron and lattice vibrations, under the action of a transverse electromagnetic radiation field. The unperturbed Hamiltonian describing the three non-interacting subsystems can be written as

$$H_0 = H_{\rm e} + H_{\rm ph} + H_{\rm F}. \tag{1}$$

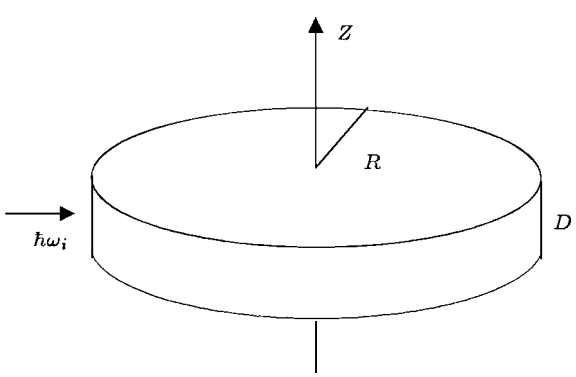


Fig.1. Geometry of a disc-like quantum dot.

The first term denotes the Hamiltonian of an electron. For simplicity, we assume that the envelope wavefunction approximation and the isotropic effective mass approximation are valid in the disc, and that the inner potential is null and the outer potential is approximately infinite. Using the cylindrical coordinates, $H_{\rm e}$ reads

$$H_{\rm e} = \begin{cases} -\dfrac{\hbar}{2m^*}\nabla^2 + V_0 & |z| \le d, \quad r \le R \\ -\dfrac{\hbar}{2m_0}\nabla^2 + V_0, & |z| > d, \quad r > R, \end{cases} \tag{2}$$

with

$$V_0 = \begin{cases} 0, & |z| \le d, \quad r \le R \\ \infty, & |z| > d, \quad r > R. \end{cases} \tag{3}$$

where m^* and m_0 are the effective mass and the free-electron rest mass of the electron, and $2d$ and R are the thickness and the radius of the disc, respectively. The second term in Eq.(1) is related to the lattice vibrations. There are different phonon modes that can exist in the QD, such as LO modes and SO modes, etc. The wave vector of the LO modes is given by[13,37]

$$\boldsymbol{K} = \boldsymbol{K}_{xy} + \boldsymbol{K}_z, \tag{4}$$

where $|\boldsymbol{K}_z| = \left(\dfrac{m\pi}{2d}\right)^2$ and $m = 1, 2, 3...$, so $|\boldsymbol{K}|_{\rm min} = \dfrac{\pi}{2d} \approx 1{\rm nm}^{-1}$, and the wave vector of a photon which participates in the Raman scattering is about $10^{-3}{\rm nm}^{-1} \ll |\boldsymbol{K}|_{\rm min}$. As the momentum conservation law must be satisfied in the Raman scattering processes, the LO phonon mode should not participate in the Raman scattering we discussed. This is different from the situation of spherical QDs.[30,31] In this paper we only concentrate our attention on the SO modes. Hence, we have

$$H_{\rm ph} = H_{\rm SO} = \sum_{\boldsymbol{q},p} \hbar\mathcal{V}_p b^+_{\boldsymbol{q},p} b_{\boldsymbol{q},p}, \tag{5}$$

where $\boldsymbol{q}$ is the wave vector, and $b^+_{\boldsymbol{q},p}$ ($b_{\boldsymbol{q},p}$) is the creation (annihilation) operator for the symmetric ($p = +1$) or antisymmetric ($p = -1$) SO mode with frequency $\mathcal{V}_p$.

The last term in Eq.(1) represents the radiation field and the photons with wave vector $\boldsymbol{k}$ and energy $\hbar\omega$,

$$H_{\rm F} = \sum_{\boldsymbol{k},\alpha} \hbar\omega(\boldsymbol{k}) a^+_\alpha(\boldsymbol{k}) a_\alpha(\boldsymbol{k}), \tag{6}$$

where $|\boldsymbol{k}| = \omega c/\eta$, c is the velocity of light in vacuum and η is the refractive index.

Thus the eigenfunction of H_0 can be written as

$$|\mu\rangle = |n_\mu\rangle_{\rm F} \, |N_\mu\rangle_{\rm SO} \, |\mu\rangle_{\rm e}\,, \tag{7}$$

where $|n_\mu\rangle_{\rm F}$ and $|N_\mu\rangle_{\rm SO}$ are, respectively, the states of the radiation field and the vibrational system, and n_μ and N_μ are the number of photons and phonons, respectively. The electronic state $|\mu\rangle_{\rm e}$ is given by [13]

$$|\mu\rangle_{\rm e} = \frac{1}{J_1(x_{0t_\mu})}\sqrt{\frac{2}{V}} J_0\left(\frac{x_{0t_\mu}}{R} r\right) \sin\frac{l_\mu \pi (z+d)}{2d}, \tag{8}$$

where V is the volume of the disc, l_μ is a positive integer and is limited by the band width, i.e. $l_\mu \le D/a$,

J_0 and J_1 are the zeroth-order and first-order Bessel functions, and x_{0t_μ} is the t_μth zero of the zero-order Bessel function, i.e. $J_0(x_{0t_\mu}) = 0$, $t_\mu = 1, 2, 3....$

The eigenenergy is expressed as

$$\varepsilon_\mu = \sum n_\mu \hbar\omega(k) + \sum N_\mu \hbar\mathcal{V}(q) + E_\mu, \tag{9}$$

with

$$E_\mu = \frac{\hbar^2}{2m^*}\left[\left(\frac{x_{0t_\mu}}{R}\right)^2 + \left(\frac{l_\mu\pi}{2d}\right)^2\right]. \tag{10}$$

On the other hand, the perturbation Hamiltonian H_I, containing the interaction terms, can be decomposed into

$$H_I = H_{\mathrm{eF}} + H_{\mathrm{e-SO}}, \tag{11}$$

where H_{eF} refers to the interaction between the electron and photon. We treat this in the dipole approximation, then for the incident radiation field

$$H_{\mathrm{eF}}(\omega_i) = j\frac{e\boldsymbol{r}\cdot\alpha_i}{\eta(\omega_i)}\sqrt{\frac{\hbar}{2V\omega_i}}[a_i^+ - a_i], \tag{12}$$

and for the secondary-radiation field

$$H_{\mathrm{eF}}(\omega_f) = j\frac{e\boldsymbol{r}\cdot\alpha_f}{\eta(\omega_f)}\sqrt{\frac{\hbar}{2V\omega_f}}[a_f^+ - a_f], \tag{13}$$

where a_γ^+ (a_γ) is the creation (annihilation) operator with the polarization vectors α_γ for photons. $\gamma = i$ denotes the incident-radiation field, and $\gamma = f$ represents the secondary-radiation photon.

Given the shape of a QD, whose radius is very large compared to the thickness, i.e. $R \gg d$, the phonon modes we adopt here are the slab phonon modes. Thus[13,37]

$$\begin{aligned} H_{\mathrm{e-SO}} =& \sum_q \mathrm{e}^{-qd}\left[\frac{sh(2qd)}{q}\right]^{1/2} \\ & \times \{B\mathrm{e}^{\mathrm{i}\boldsymbol{q}\cdot\boldsymbol{r}}[G_+(q,z)b_{q,+}^+ \\ & + G_-(q,z)b_{q,-}^+] + \mathrm{c.c.}\}, \end{aligned} \tag{14}$$

where

$$B = \mathrm{j}\left[\frac{2\pi\mathrm{e}^2}{A}\hbar\mathcal{V}_{\mathrm{LO}}\left(\epsilon_0 - \epsilon_\infty\right)\sqrt{\frac{\epsilon_\infty}{\epsilon_0}}\right]^{1/2}, \tag{15}$$

$$\begin{aligned} G_+(q,z) =& \frac{\cosh(qz)/\cosh(qd)}{(\epsilon_\infty+1) - (\epsilon_\infty-1)\mathrm{e}^{-2qd}} \\ & \times \left[\frac{(\epsilon_\infty+1) - (\epsilon_\infty-1)\mathrm{e}^{-2qd}}{(\epsilon_0+1) - (\epsilon_0-1)\mathrm{e}^{-2qd}}\right]^{1/4}, |z| \le d, \\ G_-(q,z) =& \frac{\sinh(qz)/\sinh(qd)}{(\epsilon_\infty+1) + (\epsilon_\infty-1)\mathrm{e}^{-2qd}} \\ & \times \left[\frac{(\epsilon_\infty+1) + (\epsilon_\infty-1)\mathrm{e}^{-2qd}}{(\epsilon_0+1) - (\epsilon_0-1)\mathrm{e}^{-2qd}}\right]^{1/4}, |z| \le d. \end{aligned} \tag{16}$$

Here, A is the surface area of the disc, and ϵ_0 and ϵ_∞ are the static dielectric and optical dielectric constants, respectively. $\mathcal{V}_\pm$ can be expressed in terms of the frequency of LO phonon modes

$$\mathcal{V}_\pm^2 = \left[\frac{(\epsilon_0+1) \mp (\epsilon_0-1)\mathrm{e}^{-2qd}}{(\epsilon_\infty+1) \mp (\epsilon_\infty-1)\mathrm{e}^{-2qd}}\right]\frac{\epsilon_\infty}{\epsilon_0}\mathcal{V}_{\mathrm{LO}}^2. \tag{17}$$

3. Differential cross section

There are different types of Raman scattering process. In this paper, we put emphasis on the three-step process (Stokes emission): in the first step, the system absorbs one ω_i photon from the incident radiation with the electron transition from the initial state $|i\rangle_{\mathrm{e}}$ to a virtual state $|\nu\rangle_{\mathrm{e}}$; in the second step, the electron undergoes another transition from state $|\nu\rangle_{\mathrm{e}}$ to state $|\mu\rangle_{\mathrm{e}}$ and emits an optical phonon with frequency $\mathcal{V}_f$; in the final step, the electron returns to the initial state $|i\rangle_{\mathrm{e}}$ and emits a secondary-radiation photon with frequency ω_f.

For simplicity, we assume that there is no real phonon at the initial state $|i\rangle$. It is valid in the low-temperature limit. Thus we have n_i photons with frequency ω_i, n_f photons with frequency ω_f and an electron occupying the ground state,

$$|i\rangle = |n_i + n_f\rangle_{\mathrm{F}}\,|0\rangle_{\mathrm{SO}}\,|i\rangle_{\mathrm{e}}\,, \tag{18}$$

where $|n_i + n_f\rangle_{\mathrm{F}}$, $|0\rangle_{\mathrm{SO}}$ and $|i\rangle_{\mathrm{e}}$ are the initial states of the radiation field, surface vibrational system and electron, respectively.

In the initial state

$$\varepsilon_i = n_i\hbar\omega_i + n_f\hbar\omega_f + \frac{\hbar^2}{2m^*}\left[\left(\frac{x_{01}}{R}\right)^2 + \left(\frac{\pi}{2d}\right)^2\right]. \tag{19}$$

In the final state $|f\rangle$, we have a secondary-radiation emitted photon with energy $\hbar\omega_f$, and a phonon with energy $\hbar\mathcal{V}_f$ and an electron back to the ground state. Accordingly, we have

$$|f\rangle = a^+(\omega_f)b^+(q)a(\omega_i)\,|i\rangle \tag{20}$$

and

$$\begin{aligned} \varepsilon_f =& (n_i - 1)\hbar\omega_i + (n_f+1)\hbar\omega_f + \hbar\mathcal{V}_f \\ & + \frac{\hbar^2}{2m^*}\left[\left(\frac{x_{01}}{R}\right)^2 + \left(\frac{\pi}{2d}\right)^2\right]. \end{aligned} \tag{21}$$

Based on the energy conservation law, we have $\varepsilon_i = \varepsilon_f$, hence

$$\hbar\omega_i = \hbar\omega_f + \hbar\mathcal{V}_f. \tag{22}$$

The Raman cross section can be given by the third-order perturbation theory[30,31]

$$\frac{\mathrm{d}^2\sigma}{\mathrm{d}\Omega\mathrm{d}\hbar\omega_f} = \frac{\eta(\omega_i)\eta^3(\omega_f)}{4\pi^2\hbar^4c^4}\sum_f |K_{if}|^2 (\hbar\omega_i - \hbar\mathcal{V}_f)^2. \tag{23}$$

Since the time order of quantum creation (annihilation) can be changed optionally, there are six permutations open to us, and the transition matrix elements K_{if} consist of six terms

$$K_{if} \equiv \sum_{\mu,\nu} W_{if}(\mu,\nu), \tag{24}$$

with

$$\begin{aligned} W_{if}(\mu,\nu) =& \frac{\langle f|H_{\mathrm{eF}}(\omega_f)|\mu\rangle\langle\mu|H_{\mathrm{e-SO}}|\nu\rangle\langle\nu|H_{\mathrm{eF}}(\omega_i)|i\rangle}{(\hbar\omega_i + E_i - E_\mu - \hbar\mathcal{V}_f + \mathrm{j}\hbar\Gamma_\mu)(\hbar\omega_i + E_i - E_\nu + \mathrm{j}\hbar\Gamma_\nu)} \\ &+ \frac{\langle f|H_{\mathrm{eF}}(\omega_f)|\mu\rangle\langle\mu|H_{\mathrm{eF}}(\omega_i)|\nu\rangle\langle\nu|H_{\mathrm{e-SO}}|i\rangle}{(E_i - E_\nu - \hbar\mathcal{V}_f + \mathrm{j}\hbar\Gamma_\nu)(\hbar\omega_i + E_i - E_\mu - \hbar\mathcal{V}_f + \mathrm{j}\hbar\Gamma_\mu)} \\ &+ \frac{\langle f|H_{\mathrm{e-SO}}|\mu\rangle\langle\mu|H_{\mathrm{eF}}(\omega_f)|\nu\rangle\langle\nu|H_{\mathrm{eF}}(\omega_i)|i\rangle}{(\hbar\omega_i + E_i - E_\nu + \mathrm{j}\hbar\Gamma_\nu)(E_i - E_\mu - \hbar\mathcal{V}_f + \mathrm{j}\hbar\Gamma_\mu)} \\ &+ \frac{\langle f|H_{\mathrm{eF}}(\omega_i)|\mu\rangle\langle\mu|H_{\mathrm{e-SO}}|\nu\rangle\langle\nu|H_{\mathrm{eF}}(\omega_f)|i\rangle}{(E_i - E_\nu - \hbar\omega_i + \hbar\mathcal{V}_f + \mathrm{j}\hbar\Gamma_\nu)(E_i - E_\mu - \hbar\omega_i + \mathrm{j}\hbar\Gamma_\mu)} \\ &+ \frac{\langle f|H_{\mathrm{eF}}(\omega_i)|\mu\rangle\langle\mu|H_{\mathrm{eF}}(\omega_f)|\nu\rangle\langle\nu|H_{\mathrm{e-SO}}|i\rangle}{(E_i - E_\mu - \hbar\omega_i + \mathrm{j}\hbar\Gamma_\mu)(E_i - E_\nu - \hbar\mathcal{V}_f + \mathrm{j}\hbar\Gamma_\nu)} \\ &+ \frac{\langle f|H_{\mathrm{e-SO}}|\mu\rangle\langle\mu|H_{\mathrm{eF}}(\omega_i)|\nu\rangle\langle\nu|H_{\mathrm{eF}}(\omega_f)|i\rangle}{(E_i - E_\nu - \hbar\omega_i + \hbar\mathcal{V}_f + \mathrm{j}\hbar\Gamma_\nu)(E_i - E_\mu - \hbar\mathcal{V}_f + \mathrm{j}\hbar\Gamma_\mu)}. \end{aligned} \tag{25}$$

Here, $\mathrm{j} = \sqrt{-1}$; Γ_μ and Γ_ν are the inhomogeneous line widths of the electron transitions; $\eta(\omega)$ is the refraction index as a function of radiation frequency ω; and $|\nu\rangle$ and $|\mu\rangle$ denote the intermediate states with energy levels ε_ν and ε_μ, respectively.

In the following, we calculate the matrix elements of the differential cross section. We choose the backscattering configuration, where the incident radiation wave vector is parallel to the X-axis, $\boldsymbol{k}_i \| \boldsymbol{X}$, and the scattered radiation wave vector parallel to $-X$-axis, $\boldsymbol{k}_f \| \overline{X}$, with both the polarizations of the incident and scattered wave vectors parallel to the Z-axis, $\alpha_i \| \alpha_f \| Z$, i.e. $X(Z,Z)\overline{X}$,

$$\langle\mu|H_{\mathrm{eF}}(\omega_i)|\nu\rangle = \mathrm{j}\frac{8ed}{\pi R^2}\frac{1}{\eta(\omega_i)}\sqrt{\frac{2\hbar}{\pi}\frac{n_i}{\omega_i}}\Pi_{\mu\nu}, \tag{26}$$

and

$$\langle\mu|H_{\mathrm{eF}}(\omega_f)|\nu\rangle = \mathrm{j}\frac{8ed}{\pi R^2}\frac{1}{\eta(\omega_f)}\sqrt{\frac{2\hbar}{\pi}\frac{(n_f+1)}{\omega_f}}\Pi_{\mu\nu}, \tag{27}$$

with

$$\begin{aligned} \Pi_{\mu\nu} \equiv& \frac{\omega_{\mu\nu}}{J_1(x_{0t_\mu})J_1(x_{0t_\nu})} \\ &\times \left[\frac{1}{(l_\mu - l_\nu)^2} + \frac{1}{(l_\mu + l_\nu)^2}\right] I_{t_\mu,t_\nu}, \end{aligned} \tag{28}$$

where

$$l_\mu - l_\nu = \pm 1, \pm 3, \pm 5... \tag{29}$$

We have defined

$$\begin{aligned} \omega_{\mu\nu} \equiv& \frac{E_\mu - E_\nu}{\hbar} \\ =& \frac{\hbar}{2m^*R^2}\left[\left(x_{0t_\mu} - x_{0t_\nu}\right)^2 + (l_\mu - l_\nu)^2\left(\frac{\pi R}{2d}\right)^2\right], \end{aligned} \tag{30}$$

and

$$I_{t_\mu,t_\nu} \equiv \int_0^R J_0\left(\frac{x_{0t_\mu}}{R}r\right)J_0\left(\frac{x_{0t_\nu}}{R}r\right)r\mathrm{d}r. \tag{31}$$

But

$$\langle\mu|H_{\mathrm{eF}}(\omega_i)|\nu\rangle = \langle\mu|H_{\mathrm{eF}}(\omega_f)|\nu\rangle = 0, \tag{32}$$

with

$$l_\mu - l_\nu = 0, \pm 2, \pm 4... \tag{33}$$

On the other hand,

$$\langle\mu|H_{\mathrm{e-SO}}|\nu\rangle = \frac{2B}{R^2d}T_{\mu\nu}(q,d), \tag{34}$$

where

$$\begin{aligned} & T_{\mu\nu}(q,d) \\ =& \frac{\exp[-qd]}{J_1(x_{0t_\mu})J_1(x_{0t_\nu})}\frac{\sinh(qd)}{\cosh(qd)}\left[\frac{\sinh(2qd)}{q}\right]^{1/2} J_{t_\mu,t_\nu} \\ &\times \left\{\frac{q}{q^2 + \left[(l_\nu - l_\mu)\dfrac{\pi}{2d}\right]^2} - \frac{q}{q^2 + \left[(l_\nu + l_\mu)\dfrac{\pi}{2d}\right]^2}\right\} \\ &\times [(\epsilon_\infty + 1) - (\epsilon_\infty - 1)\exp(-2qd)]^{-3/4} \\ &\times [(\epsilon_0 + 1) - (\epsilon_0 - 1)\exp(-2qd)]^{-1/4}, \end{aligned} \tag{35}$$

with

$$J_{t_\mu,t_\nu} \equiv \int_0^R J_0(qr) J_0\left(\frac{x_{0t_\mu}}{R} r\right) J_0\left(\frac{x_{0t_\nu}}{R} r\right) r\mathrm{d}r, \quad (36)$$

$$l_\mu - l_\nu = 0, \pm 2, \pm 4... \quad (37)$$

and

$$\langle \mu | H_{\mathrm{e-SO}} | \nu \rangle = 0, \quad (38)$$

with

$$l_\mu - l_\nu = \pm 1, \pm 3, \pm 5... \quad (39)$$

It is obvious that the antisymmetric SO modes are inhibited in the Raman scattering process according to Eqs.(14), (38) and (39). Also, it is clearly seen that the selection rules Eqs.(29) and (37) must be satisfied if the Raman cross section is not equal to zero.

After cumbersome calculations we obtain the expressions for the differential cross section for the three-step Raman scattering process

$$\begin{aligned} \frac{\mathrm{d}^2\sigma}{\mathrm{d}\Omega \mathrm{d}\omega_f} =& \frac{2048}{\pi^8 c^4} \frac{\mathrm{e}^6 d^2}{R^{14}\hbar^3} (\epsilon_0 - \epsilon_\infty) \\ & \times \sqrt{\frac{\epsilon_\infty}{\epsilon_0}} \frac{\eta(\omega_f)}{\eta(\omega_i)} \frac{(\omega_i - \mathcal{V}_f)\mathcal{V}_{\mathrm{LO}}}{\omega_i} \\ & \times n_i(n_f+1) \left| \sum_{\mu,\nu} \Lambda_{\mu\nu} \right|^2, \end{aligned} \quad (40)$$

where we have made use of the relationship between ω_f and ω_i, based on the momentum conservation law

$$q = \left\{ \left(\frac{\eta(\omega_f)^2}{c^2} \right) \mathcal{V}_f^2 + 2 |\boldsymbol{k}_f| |\boldsymbol{k}_i| (1 - \cos\beta) \right\}^{1/2}. \quad (41)$$

Here $\boldsymbol{k}_i$ and $\boldsymbol{k}_f$ are, respectively, the wave vectors of the incident radiation and secondary radiation field, and β is the angle between $\boldsymbol{k}_i$ and $\boldsymbol{k}_f$, with

$$\begin{aligned} \omega_i =& c|\boldsymbol{k}_i| / \eta(\omega_i), \\ \omega_f =& c|\boldsymbol{k}_f| / \eta(\omega_f). \end{aligned} \quad (42)$$

We have

$$\begin{aligned} \Lambda_{\mu\nu} =& \frac{\Pi_{f\mu} T_{\mu\nu}(q,d) \Pi_{\nu i}}{(\omega_i - \omega_{\nu i} + \mathrm{j}\Gamma_\nu)(\omega_i - \mathcal{V}_f - \omega_{\mu i} + \mathrm{j}\Gamma_\mu)} \\ & - \frac{\Pi_{f\mu} \Pi_{\mu\nu} T_{\nu i}(q,d)}{(\omega_{\nu_i} + \mathcal{V}_f - \mathrm{j}\Gamma_\nu)(\omega_i - \mathcal{V}_f - \omega_{\mu i} + \mathrm{j}\Gamma_\mu)} \\ & - \frac{T_{f\mu}(q,d) \Pi_{\mu\nu} \Pi_{\nu i}}{(\omega_i - \omega_{\nu i} + \mathrm{j}\Gamma_\nu)(\omega_{\mu i} + \mathcal{V}_f - \mathrm{j}\Gamma_\mu)} \\ & + \text{three similar terms.} \end{aligned} \quad (43)$$

Compared to the first three terms, the contribution of the last three terms in Eq.(43) is so small that it can be neglected. In the present work, we thus consider just the contribution of the first three terms of Eq.(43) during the calculation of $\Lambda_{\mu\nu}$ for the determination of the differential cross section.

4. Results and discussion

In this section, the resonant differential cross section given by Eqs.(40) and (43) is calculated numerically for a GaAs QD. The parameters used in the computation are:[13] ϵ_0=13.18, ϵ_∞=10.89, $\hbar\omega_{\mathrm{LO}}$=36.25meV, and the lattice constant a = 0.56533nm. The effective mass of an electron is taken to be $m^* = 0.067m_0$. The relaxation parameters Γ are not well identified experimentally even in bulk materials. We use the following values for the purpose of order estimation:[38] $1/\Gamma_a = 1/\Gamma_b$=1ps.

In Fig.2 we plot the differential cross section as a function of the incident phonon energy $\hbar\omega_i$. The thickness and the radius of the disc are kept at 6 nm and 50 nm, respectively. The number of photons in the initial states is $n_i = 1$, $n_f \ll 1$. It can be seen from Eqs.(43) and (40) that the differential cross section $\dfrac{\mathrm{d}^2\sigma}{\mathrm{d}\Omega \mathrm{d}\omega_f}$ shows a maximum

$$\omega_i - \mathcal{V}_f = \omega_{\mu i}, \quad (44)$$

or

$$\omega_i = \omega_{\nu i}. \quad (45)$$

So we can obtain the information about phonons and electronic states involved in the scattering process. Figure 2 also demonstrates that there are several double peaks, such as (a, A), (b, B) and (c, C) in the Raman profiles. Peaks a, b and c are related to the incoming resonance, and the incident photon energy corresponds to the transition, namely, Eq.(45) is fulfilled. Peaks A, B and C are related to the outgoing resonance, i.e. the scattering photon is in resonance and Eq.(44) is fulfilled. The incoming resonance is larger than the outgoing resonance at (a, A). In contrast, the outgoing resonance is larger than the incoming resonance at (b, B) and (c, C). This shows that the incoming resonance dominates for transitions to lower energy states and the outgoing resonance dominates for transitions to higher energy states.

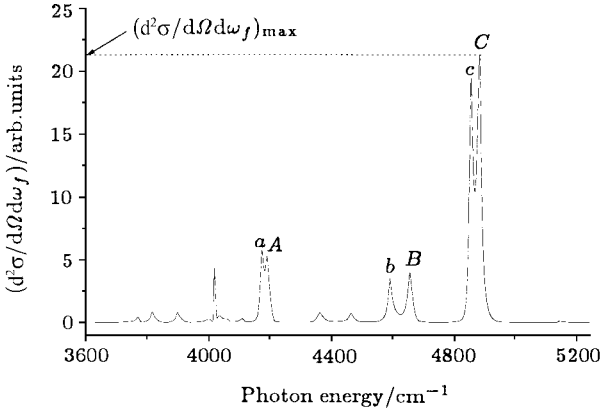


Fig.2. Raman differential cross section as a function of incident photon energy for a GaAs quantum disc with D=6nm and R=50nm in the $X(Z,Z)\overline{X}$ scattering configurations.

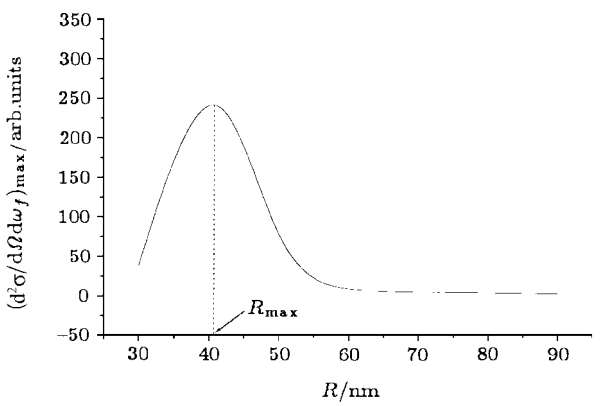


Fig.3. The maximum value of the differential cross section as a function of the radius for a GaAs quantum disc with thickness D=3.36nm in the $X(Z,Z)\overline{X}$ scattering configurations.

It is also clearly seen that the differential cross section reaches the maximum $\left(\frac{d^2\sigma}{d\Omega d\omega_f}\right)_{max}$ at point C in Fig.2. $\left(\frac{d^2\sigma}{d\Omega d\omega_f}\right)_{max}$ has something to do with the disc radius R and thickness D. Figure 3 shows the $\left(\frac{d^2\sigma}{d\Omega d\omega_f}\right)_{max}$ versus the disc radius R, while the disc thickness D is fixed at 3.36nm. There is a peak at point R_{max}. This demonstrates that $\left(\frac{d^2\sigma}{d\Omega d\omega_f}\right)_{max}$ increases with the radius R when $R \leq R_{max}$; but $\left(\frac{d^2\sigma}{d\Omega d\omega_f}\right)_{max}$ decreases as the radius increases when $R > R_{max}$. Figure 4 shows $\left(\frac{d^2\sigma}{d\Omega d\omega_f}\right)_{max}$ versus thickness D, while the radius R is fixed at 50nm. There is also a peak at point D_{max}. Since electrons are considered to be confined in a QD with infinite potential barriers, the spatial overlap between two bound states is dependent on the disc radius R and thickness D. The spatial overlap is optimum at R_{max} and D_{max}, leading to the matrix elements in Eqs.(26) and (27), and consequently the differential cross section $\frac{d^2\sigma}{d\Omega d\omega_f}$ reaches the maximum.

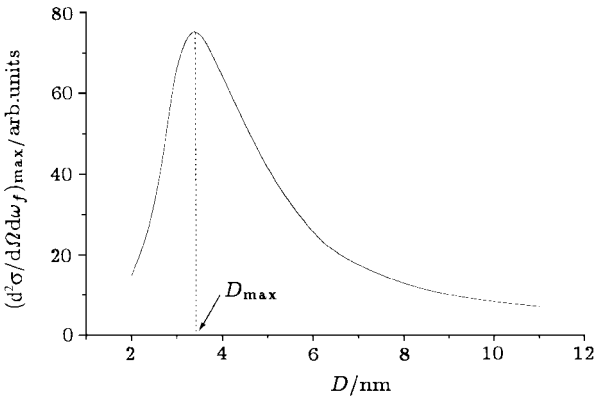


Fig.4. The maximum value of the differential cross section as a function of the thickness for a GaAs quantum disc with radius R=50nm in the $X(Z,Z)\overline{X}$ scattering configurations.

Finally, according to Eq.(40) we should note that the differential cross section is proportional to n_f+1. If $n_f \gg 1$, the scattering photon with frequency ω_f will be the main part in the secondary-radiation field. So, stimulated Raman scattering can be realized in our system.

5. Conclusions

We have investigated theoretically the differential cross section for the electron Raman scattering process involving SO phonon-assisted transitions in a semiconductor QD. It is shown that the antisymmetric SO mode is inhibited in the Raman process. The numerical results in the scattering configuration $X(Z,Z)\overline{X}$ also show that the differential cross section depends on the disc radius, thickness and the energy of the incident radiation field. We can obtain information about the phonon mode and the intermediate electronic states involved in the scattering process forming the Raman peaks. Moreover, the system studied is expected to be a stimulated Raman scattering laser model. So far as we know, there are few experimental results about this type of Raman scattering. We hope that our results can stimulate interest in experimental efforts in this direction.

References

[1] Banfi G P and Degiorgio V 1998 *Adv. Phys.* **47** 447
[2] Yoffe A D 2001 *Adv. Phys.* **50** 1
[3] Yoff A D 1993 *Adv. Phys.* **42** 173
[4] Zhang A Z, Zhang P, Duan S Q, Zhao X G and Liang J Q 2001 *Chin. Phys.* **10** 537
[5] Hui P 2000 *Chin. Phys.* **9** 844
[6] Boucaud P, Thanh V L, Sauvage S, Débarre D and Bouchier D 1999 *Appl. Phys. Lett.* **73** 401
[7] Wang Z B, Wu F L, Chen Q H and Jiao Z K 2001 *Chin. Phys.* **10** 437
[8] Brunhes T, Boucaud P and Sauvage S 2000 *Phys. Rev.* B **61** 5562
[9] Xu X H, Jiang H, Fu R T and Sun X 2000 *Acta Phys. Sin.* **49** 426 (in Chinese)
[10] Pan L X, Li S S and Xia J B 2001 *Chin. Phys.* **10** 655
[11] Jacak L, Hawpycak P and WóJs A 1998 *Quantum Dots* (Berlin: Spring-Verlag) p6
[12] Harrison P 1999 *Quantum Wells, Wires and Dots* (New York: Wiley) p 2
[13] Chen C Y, Li W S, Teng X Y and Liang S D 1998 *Physica* B **245** 92
[14] Roca E, Trallero-Giner C and Cardona M 1994 *Phys. Rev.* B **49** 13704
[15] Reed M A, Randall J N, Aggarwal R J, Matyi R J, Moore T M and Wetsel A E 1988 *Phys. Rev. Lett.* **60** 535
[16] Kraus J, Weimann G and Panzlaff K 1995 *J. Phys.: Condens. Matter* **7** 7761
[17] Chen C Y, Li W S and Yeung H K 1998 *Solid State Commun.* **106** 341
[18] Bockelmann U and Bastard G 1990 *Phys. Rev.* B **42** 8947
[19] Nomura S 1992 *Phys. Rev.* B **45** 1305
[20] Bergues J M, Betancourt-Riera R, Riera R and Marín J L 2000 *J. Phys.: Condens. Matter* **12** 7983
[21] Zucker J E, Pinczuk A and Chemla D S 1988 *Phys. Rev.* B **38** 4287
[22] Cros A, Cantarero A, Trallero-Giner C and Cardona M 1992 *Phys. Rev.* B **46** 12627
[23] Shields A J, Trallero-Giner C, Cardona M, Grahn H T, Ploog K Haisler V A, Tenne D A, Moshegov N T and Toropov A I 1992 *Phys. Rev.* B **46** 6990
[24] Krauss T D and Wise F W 1997 *Phys. Rev.* B **55** 9860
[25] Sood A K, Menéndez J, Cardona M and Ploog K 1985 *Phys. Rev. Lett.* **54** 2115
[26] Sood A K, Menéndez J, Cardona M and Ploog K 1985 *Phys. Rev. Lett.* **54** 2111
[27] Hayashi S and Kanamori H 1982 *Phys. Rev.* B **26** 7079
[28] Liu F, Liao L S, Wang G H, Cheng G X and Bao X M 1996 *Phys. Rev. Lett.* **76** 604
[29] Heitz R, Mukhametzhanov I, Stier O, Madhukar A and Bimberg D 1999 *Phys. Rev. Lett.* **83** 4654
[30] Menendez E, Trallero-Giner C and Cardona M 1997 *Phys. Status Solidi* b **199** 81
[31] Chamberlain M P, Trallero-Giner C and Cardona M 1995 *Phys. Rev.* B **51** 1680
[32] Marini J C, Stebe B and Kartheuser E 1994 *Phys. Rev.* B **50** 14302
[33] Krauss T D and Wise F W 1997 *Phys. Rev.* B **55** 9860
[34] Scamarcio G, Spagnolo V, Ventruti G and Lugará M 1996 *Phys. Rev.* B **53** R10489
[35] Kanschke W, Sood A K, Cardona M, Ploog K, Haisler V A, Tenne D A, Moshegov N T and Toropov A I 1987 *Phys. Rev.* B **36** 1612
[36] Xu J F, Cheng G X, Yang W and Du Y 1996 *J. Phys. B: At. Mol. Opt. Phys.* **29** 6227
[37] Licari J J and Evrard R 1977 *Phys. Rev.* B **15** 2254
[38] Takagahara T 1989 *Phys. Rev.* B **39** 10206